Ab initio Investigation of Elasticity and Stability of Aluminium

Weixue Li   Tzuchiang Wang

LNM, Institute of Mechanics, Chinese Academy of Science,

Beijing, 100080, China

Abstract

On the basis of the pseudopotential plane-wave(PP-PW) method in combination with the local-density-functional theory(LDFT), complete stress-strain curves for the uniaxial loading and uniaxial deformation along the [001] and [111] directions, and the biaxial proportional extension along [010] and [001] of aluminium are obtained. During the uniaxial loading, certain general behaviors of energy versus stretch and the load versus the stretch are confirmed; in each acse, there exist three special unstressed structures: f.c.c., b.c.c. and f.c.t. for [001]; f.c.c., s.c. and b.c.c. for [111]. Using stability criteria, we find that all of these state are unstable, and always occur together with shear instability, except the natural f.c.c. structure. A Bain transformation from the stable f.c.c. structure to the stable b.c.c. configuration cannot be obtained by uniaxial compression along any equivalent [001] and [111] direction. The tensile strength are similar for the two directions. For the higher energy barrier of [111] direction, the compressive strength is greater than that for the [001] direction. With increase in the ratio of the biaxial proportional extension, the stress and tensile strength increase; however, the critical strain does not change significantly. Our results add to the existing *ab initio* database for use in fitting and testing interatomic potentials.

62.20.-x, 62.20.Dc, 62.20.Fe, 81.40.Jj

Typeset using REVTEX

1

I. INTRODUCTION

Investigation of elastic behavior of perfect single crystal under loading is of interest. It can, for example, be carried out on a system in which substantial, elastic (but not necessary linear) deformation may occur, in that case substantial deformation may occur either without significant dislocation movement or before deformation caused by dislocation movement become dominant. Deformation of whisker, twinning and martensitic transformations are relevant examples. The instability and branching under loading is related to ideal strength and transformation. Such information is very useful in the analysis of structural response in solids, *e.g.* polymorphism, amorphization, and melting to fracture.

Although Born [1] criteria are widely used in the investigation of strength, they are only valid under zero load. On the basis of a series of comprehensive theoretical and computational studies, Hill and Milstein [2]-[7] pointed out the following: (i): stability is relative and coordinate dependent;and (ii) different choices of strain measure lead to different domains of stability. On the basis of the Morse potential, they investigated the mechanical response of perfect crystal, which included the stress-strain relation, instability, branching and the strength of f.c.c. Cu [8], f.c.c. Ni [10], [11], [12],and α-Fe [9], for different loading modes (*e.g.* uniaxial loading, uniaxial deformation, and shear loading. here, 'uniaxial loading' means that uniaxial stress is applied to one axis, and the lateral face is relaxed and stress-free(traction-free), while 'uniaxial deformation' just means that one axis is dilated or contracted, and the dimension of other two axes are fixed; in uniaxial deformation, all three axes are subjected to loading.) The loading direction which were adopted included [001], [110] and [111]. Possible branching path were revealed. Using the thermodynamics Gibbs function, Wang *et al* [13], [14] developed an equivalent-stability analysis method, and investigated the onset of instability in a homogeneous lattice under critical loading. The onset modes, derived from the stability criteria, were verified by means of a molecular dynamics simulation. Zhou and Joós [15] derived general expressions for the stability criteria by an appropriate thermodynamics potential.

There has been less investigation based on first principle. Senoo *et al* [16] discussed the elastic deformation due to [100] loading of Al, using the pseudopotential method. Esposito *et al* [17] dealt with the tensile strength of f.c.c. Cu under uniaxial deformation on the basis of the *ab initio* potential, augmented-spherical-wave(ASW), KKR methods. However, relaxation of the crystal structure was not permitted. Paxton *et al* [18] calculated the theoretical strength of five b.c.c. transition metal, and Ir, Cu, and Al by considering ideal-twin stresses using the full-potential linear muffin-tin orbital (FP-LMTO). Sob *et al.* [19] investigated the theoretical tensile stress in tungsten single crystal under [001] and [111] loading by the FP-LMTO method. The stability analysis was not explicit in any of the above cases.

Bain transformation takes a crystal from its stable b.c.c. configuration into a stable f.c.c. structure, and vice versa, by means of homogeneous axial deformations. Which path requires the lowest energy and stress barrier between these states was investigated and reviewed by Milstein *et al.* [20]. The general mechanics and energetics of the Bain transformation were presented. On the basis of the empirical pseudopotential, Milstein *et al.* [20] investigated the Bain transformation of crystalline sodium in detail. These kind of transformation is also relevant to the investigation of epitaxial thin film [21].

In this paper, we present a direct investigation on the elasticity, the stress-strain relation, the stability, and the ideal strength of f.c.c. Aluminium within density functional theory. The stability analysis is considered explicitly, on the basis of the theory of Hill, Milstein [2], [3], [7] and Wang *et al.* [13], [14]. We consider several loading modes: uniaxial deformation and uniaxial loading along the [001] and [111] directions, and biaxial proportional extension along [001] and [010]. The deformation is homogeneous, elastic, and permitted to be appropriately large. The stress-strain relation are calculated, and the ideal strength is approached via the loss of stability. Branching or structure transformation from a primary path of deformation takes place with the loss or exchange of stability, which are relevant to the Bain transformation. In this way, the mechanical responses for different loading modes and direction are obtained, clearly from first principle,.

The paper is organized as follows. The calculation model is presented in Sec. 2. In this section, we give the formulation of stress, elastic stiffness coefficients, and stability criteria, especially for three loading modes. Numerical precision is evaluated at the end of this section. As a benchmark, equilibrium properties and elastic constants are calculated in the Sec. 3, [001] uniaxial deformation and [001] uniaxial loading are considered in Sec. 4, and a stability analysis is implemented. In Sec. 5, [111] uniaxial deformation and [111] uniaxial loading are considered. Results on the biaxial proportional extension are given in Sec. 6. *Ab initio* calculations can be used to construct a database for fitting and testing interatomic potential [22], [23]; a brief discussion of our results together with the existing *ab initio* database for aluminium is given in Sec. 7. A summary and conclusions are presented in the last section.

II. FORMULATION

Consider an initial unstressed and unstrained configuration, denoted as $\mathbf{X_0}$. It undergoes homogeneous deformation under a uniform applied load, and changes from $\mathbf{X_0}$ to $\mathbf{X} = \mathbf{J}\mathbf{X_0}$, where $\mathbf{J}$ is the deformation gradient or the Jacobian matrix and the rotation part is subtracted. The associated Lagrangian strain tensor $\mathbf{E}$ is:

$$\mathbf{E} = \frac{1}{2}(\mathbf{J^T}\mathbf{J} - \mathbf{I}) \tag{1}$$

and the physical strain is:

$$\mathbf{e} = (\mathbf{J^T}\mathbf{J})^{\frac{1}{2}} - \mathbf{I} \tag{2}$$

For the present deformation, internal energy U is rotationally invariant and therefore only a function of $\mathbf{E}$. The second Piloa-Kirchhoff stress tensor $\mathbf{T}$ [24] is defined as:

$$T_{ij} = \frac{1}{V_0}\frac{\partial U}{\partial E_{ij}} \tag{3}$$

It relates Cauchy stress, *i.e.*, true stress τ_{kl} , by the following equation:

$$T_{ij} = det|\mathbf{J}| J_{ik}^{-1} J_{jl}^{-1} \tau_{kl} \tag{4}$$

where $det|\mathbf{J}|$ is the ratio V/V_0. With the Cauchy stress, the applied force can be obtained by multiplying by the current transverse area.

For the stressed state $\mathbf{X}$, the elastic constants are determined through the equation:

$$C_{ijkl}(\mathbf{X}) = \frac{1}{V(\mathbf{X})} \left(\frac{\partial^2 U}{\partial E'_{ij} \partial E'_{kl}} \Big|_{E'=0} \right) \tag{5}$$

where $\mathbf{E}'$ is Lagrangian strain around the state $\mathbf{X}$. These elastic constants are symmetric with respect to interchange of indices, and are often expressed in condensed Voigt notation.

To analyse the stability, the elastic stiffness coefficient $\mathbf{B}$ [14] is introduced as follows:

$$B_{ijkl} = C_{ijkl} + \frac{1}{2} (\delta_{ik}\tau_{jl} + \delta_{jk}\tau_{il} + \delta_{il}\tau_{jk} + \delta_{jl}\tau_{ik} - 2\delta_{kl}\tau_{ij}) \tag{6}$$

From this definition, we can see that $\mathbf{B}$ does not posses $(ij) \longleftrightarrow (kl)$ symmetry generally. The system may be unstable when

$$det|\mathbf{B}| = 0 \tag{7}$$

for the first time.

The following loading modes are considered:

(i) Uniaxial Deformation.

$$e_{ij} = e\delta_{i3}\delta_{j3} \qquad i, j = 1, 2, 3 \tag{8}$$

In this mode, a strain is specified, and strain energy is evaluated by subtracting a reference energy, which is calculated using the theoretical lattice constant, on the basis of a total energy calculation. The corresponding stretches of three axes are: $\lambda_1 = \lambda_2 = 1$, $\lambda_3 < 1$ for compression, and $\lambda_3 > 1$ for tension.

(ii) Uniaxial Loading.

$$\tau_{ij} = \sigma\delta_{i3}\delta_{j3} \qquad i, j = 1, 2, 3 \tag{9}$$

For a given longitudinal strain, let transverse lattice contract or dilate to make the total energy arriving a minimum, which corresponds zero stress(traction) on lateral faces. Due to

5

the crystal symmetry, the transverse contraction or dilation is same in the two transverse directions. With the longitudinal strain and corresponding transverse strain, the strain energy of the uniaxial loading is calculated. The corresponding stretches of three axes are: for compression, $\lambda_1 = \lambda_2 > 1$, and $\lambda_3 < 1$; for tension, $\lambda_1 = \lambda_2 < 1$, and $\lambda_3 > 1$.

(iii) Biaxial Proportional Extension

$$e_{22} = \alpha e_{33} \ne 0 \quad e_{ij} = 0 \quad otherwise \tag{10}$$

Ab initio pseudopotential plane-wave method is implemented. On the basis of the mechanism of Hamman [28] and Troullier and Martins [29], soft first principle pseudopotentials are generated using the package DgncppB [25], [26]. The package Fhi96md [27] , which employs a first-principle pseudopotential and a plane-wave basis set, is used to perform the DFT total-energy calculation. In our calculations, local density approximation(LDA) with the exchange and correlation energy functional developed by Perdew and Zunger [30] is adopted.

Two supercell are designed in our calculations: one is four-atom supercell, for use in considering the equilibrium properties and elastic constants, uniaxial deformation and loading along [001], and biaxial deformation along [010] and [001]; the other one is three-atom supercell for use in considering uniaxial deformation and loading along [111]. Due to the calculation of stress and elastic constants, the precision must be evaluated carefully. E_{cut}=12Ry is sufficient in our pseudopotential plane-wave calculations. Due to discontinuous feature of occupation number of metal electron, a large number of k-space samples must be used to reach sufficient precision. A smear parameter Δ is introduced to decrease the number of k-points. Our calculation show that $\Delta = 0.058Ry$ already gives a satisfactory result. The corresponding k-meshes are $8 \times 8 \times 8$ for the four-atom supercell, and $10 \times 10 \times 6$ for three-atom supercell.

III. EQUILIBRIUM PROPERTIES AND ELASTIC CONSTANTS

As a test, we have calculated the equilibrium lattice constant and elastic constants of bulk Al. Face-centered-cubic Al has three independent elastic constant, *i.e.* C_{11}, C_{12}, C_{44}.

The equilibrium lattice constants a_0 the bulk modulus B_0 are obtained by fitting energy-volume curve to Murnaghan equation of state. [31] The relation between bulk modulus B_0 and elastic constant is $B_0 = (C_{11} + 2C_{12})/3$. From the uniaxial deformation along [001] direction and trigonal strain along [111] direction, C_{11} and C_{44} are obtained. The result are given in table 1.

The theoretical lattice constant, $a_0 = 3.97\mathring{A}$, is 2% smaller than experimental value $a_0 = 4.05\mathring{A}$, and the corresponding elastic constants are 10% larger than experimental values [32] measured at room temperature. This difference is typical of DFT-LDA calculations, and can be see clearly from other first principle results. Sun et $al.$ [33] pointed out the elastic constants are sensitive to the lattice constant of the crystal, and calculated the corresponding data using the lattice constants at room temperature. On the basis of the linear augmented plane wave(LAPW) method, Mehl and Klein [34] made similar calculations, and gave the Bulk modulus, Young's modulus, shear modulus, average Possion ratio and anisotropy of isotropic materials with an orientation average. We also calculated the elastic moduli using the experimental lattice constants, we present the results in table 1. All of the theoretical calculations are in good agreement with experimental data, and better result are given by our calculation. However, it is worthy noting that we performed our calculations of the strength and stability using the theoretical lattice constant. Any externally imposed strain and stress should be excluded to get accurate results.

IV. [001] UNIAXIAL LOADING AND [001] UNIAXIAL DEFORMATION

A four-atom face-centred tetragonal supercell was designed for investigating [001] uniaxial loading and [001] uniaxial deformation. [100], [010] and [001] is selected as X-, Y- and Z-axis. In the initial equilibrium state, the f.c.t. structure is f.c.c. With the same f.c.t. cell, b.c.t. cell can be got by means of an axial rotation by $\frac{\pi}{4}$ around [001] axial. This relation can be found from figure 1. We start from the unstressed f.c.c. state where $\lambda_1 = \lambda_2 = \lambda_3 = 1$, and let the Z-axis be compressed: on the prescribed path, the lattice must pass through the state

$\lambda_3 = \lambda_1/\sqrt{2} = \lambda_2/\sqrt{2}$ where the b.c.t. becomes a b.c.c. one. The cubic symmetry at this point implies that the loads are hydrostatic. For [001] uniaxial loading, in particular, since the transverse loads are always zero, the axial load at this state must be zero. Since the load must be tensile as $\lambda_3 \to \infty$ and compressive as $\lambda_3 \to 0$, the existence of two unstressed states on the primary path of [001] loading implies a third zero point in general. Obviously, the third one does not have any symmetry higher than tetragonal. The state located in the central unstressed position is always unstable at its local energy maximum. For a detailed analysis and proof of the general form of the energy versus stretch and stress versus stretch, the reader is referred to the original paper of Milstein [35], [36].

For tetragonal symmetry of the crystal under uniaxial loading and uniaxial deformation along the [001] direction, the number of independent elastic constants is reduced to six: C_{33}, C_{12}, $C_{13} = C_{23}$, $C_{11} = C_{22}$, $C_{44} = C_{55}$ and C_{66}; all of the other C_{ij} are equal to zero. Since we are more interested in uniaxial loading, we analyse its stability. With Eq. 6, 7 and 9, we write the instability criteria of [001] uniaxial loading as follows:

$$(C_{33} + \sigma)(C_{11} + C_{12}) - 2C_{13}(C_{13} - \sigma) \leq 0 \tag{11}$$

$$C_{11} - C_{12} \leq 0 \tag{12}$$

$$C_{44} + \frac{1}{2}\sigma \leq 0 \tag{13}$$

$$C_{66} \leq 0 \tag{14}$$

The first expression involves the vanishing of the bulk modulus, and is referred to as the spinodal instability criterion. The second instability involves symmetry breaking (bifurcation) with volume conservation; it may be identified as the tetragonal shear breaking, and is referred to as Born instability. In this case, the crystal can branch from the tetragonal path to a face-centred orthorhombic path under uniaxial dead loading; that is, the branching is $\delta\lambda_1 = -\delta\lambda_2 \neq 0$ with $\delta\lambda_3 = 0$ and $\delta\tau_{11} = \delta\tau_{22} = \delta\tau_{33} = 0$. The condition $C_{66} = 0$, when the C_{ij} are reckoned relative to the f.c.t. crystal axes, is equivalent to $C_{11} - C_{12} = 0$ when the C_{ij} are computed relative to the axes of the b.c.t.cell. So, for the state where $C_{66} = 0$(referred to the f.c.t. axes), the tetragonal crystal branch to a body-centred orthorhombic path under

uniaxial loading. $C_{44} + \frac{1}{2}\sigma = 0$ gives another shear instability.

Energy versus strain and stress, force versus strain curve are given in figure 2 (unless otherwise stated, the strain, force and stress, given in figures are the physical strain, applied force, and Cauchy stress.) There exist only one energy minimum under uniaxial deformation. Any departure from the minimum for this loading mode lead to a rapid increase of the strain energy. Due to the triaxial stresses for the uniaxial deformation, its strain energy is always greater than that for the uniaxial loading. This is same as the Milstein's conclusion: the uniaxial loading represents the lowest-energy path between any two Bain paths. However, another local maximum and local minimum state are found under uniaxial compression. The longitudinal and transverse strain at the local maximum are $e_{33} = -0.20$ and $e_{11} = 0.1313$ respectively; the ratio of stretch $(1 - 0.2)/(1 + 0.1313) = 0.7071$, is approximately equal to $1/\sqrt{2}$. The corresponding structure is b.c.c. with lattice constant $3.176\mathring{A}$, as expected. The remaining local minimum is a f.c.t. structure with $e_{33} = -0.305$. From figure2(b), we see that all three extreme are stress-free. Because b.c.c. is located at a local maximum, it is unstable.

The elastic constants and corresponding stability range under [001] uniaxial loading are shown in figure 3. C_{66} is always negative over the range [-0.40, -0.128], which includes the un-stressed f.c.t. state. That means that, although the stress-free f.c.t. is at the local minimum of the uniaxial loading , it is still unstable against shear loading. On the basis of the explanation of C_{66}, we wee that this f.c.t. state can transform to a body-centred orthorhombic under uniaxial compression. The range of spinodal instability under compression is [-0.263, -0.119]. The b.c.c. state lies at a double instability.

From figure 2(b), the compressive strength of the [001] uniaxial loading is -5.62 GPa with $e_{33} = -0.1$. During tension, the stress approaches its maximum 12.54 GPa with $e_{33} = 0.36$. However, $C_{11} - C_{12}$ and $C_{44} + \frac{1}{2}\sigma$ have already become negative when e_{33} exceeded 0.272, and the corresponding stress is 12.1 GPa. This gives the lower limit of the tensile strength. Two possible branching are triggered at this critical strain. With $C_{11} - C_{12} = 0$, tetragonal lattice will transform via a face-centred orthorhombic path and finally become a stable b.c.c.

state at last [37]. With $C_{44} + \frac{1}{2}\sigma = 0$, the orthorhombic symmetry will be lost. However, which branching takes place depends on the higher-order elastic modulus. By means of pseudopotential methods based on a proposed model potential, Senoo *et al.* [16] obtained a compressive strength of approximately -5.0 GPa, with strain -0.11, and unstressed b.c.c. structure occurred at a strain of -0.2. These results are very similar to ours. However, the tensile strength, which they obtained, 17.4 GPa with a strain of 0.42, is greater than ours. The $C_{11} - C_{12} = 0$ branching was assumed to take place at a strain 0.15 in their work. Paxton *et al.* [18] calculated the ideal-twin stress of Al on the basis of the FP-LMTO method. The corresponding value, $0.14 \times \frac{1}{3}(C_{11} - C_{12} + C_{44}) = 4.61$ GPa (here the C_{ij} are the elastic constants of theoretical lattice), is approximately one third of our tensile strength.

Unlike the findings for Ni [10], [11], [12] and Cu [8], α-Fe [9] calculated by Milstein *et al.*, the uniaxial stress and force of Al are always lower than those for uniaxial deformation before they approach the maximum. The transverse strain versus longitudinal strain is given in figure 4, and the corresponding Possion ratio is positive along the whole path of uniaxial loading.

V. [111] UNIAXIAL LOADING AND [111] UNIAXIAL DEFORMATION

For the case of [111] uniaxial loading and [111] uniaxial deformation, the supercell is designed as follows: the planar vectors are identical to two primitive f.c.c. lattice vectors, for instance along [110] and [101] directions; the third lattice vectors is in the [111] direction; and here we select three layers. In each layer, there is only one atom.

The path of deformation considered is axisymmetric, and all directions transverse to [111] are equally stretched or fixed. The axisymmetric path of deformation under [111] loading and [111] deformation consequently passes through three cubic configurations: f.c.c., s.c. and b.c.c. with increase of the compression. To illustrate this, a single quantity, r, the ratio of the longitudinal to the transverse stretch under loading, is defined. Three smallest tetrahedra are cut separately from f.c.c., s.c., and b.c.c. as shown in figure 5. The bottom

plane ABC is just the {111} plane, and the direction of OD is [111]. The ratios of height and edge length of bottom plane are $\frac{\sqrt{6}}{3}$, $\frac{\sqrt{6}}{6}$, $\frac{\sqrt{6}}{12}$, *i.e.* 1, 0.5, 0.25. These ratios are just values of r, which we define above. When r decreases from 1 to 0.25 during compression, the cubic f.c.c., s.c. and b.c.c. structures appear in turn. The details can be found from figure 5. During [111] uniaxial loading, the transverse load is always zero, and cubic symmetry requires three cubic configurations to be stress-free. However, during [111] uniaxial deformation, there is always exist a transverse load, and cubic symmetry of s.c. and b.c.c. indicates hydrostatic compression. For the transverse contraction under [111] loading, the s.c. and b.c.c. states will occur earlier than the [111] deformation.

The calculated results are given in figure 6. Just like in the [001] case, there exist only one minimum under uniaxial deformation, and the strain energy is always higher than the uniaxial loading. Under uniaxial loading, another local maximum and local minimum are obtained; the form of energy versus stretch relation is just same as for [001] loading. From figure 4, we get $e_{33} = -0.333$ at the local maximum point with $e_{11} = -0.334$; the corresponding r, 0.5, is simply that for the unstressed s.c. configuration. This state is unstable because it is located at a local energy maximum. At the local minimum, $e_{33} = -0.59$ and $e_{11} = 0.64$; the corresponding r, 0.25, is that for unstressed b.c.c. structure. From a simple geometric calculation, we obtain the lattice constant of stress-free s.c. and b.c.c. structures: 2.648Å and 3.253Å respectively. The corresponding elastic constants are: (s.c.) $C_{11} + C_{12} = -10.1$ GPa, $C_{11} - C_{12} = -24.9$ GPa and $C_{44} = 4.4$ GPa; (b.c.c.) $C_{11} + C_{12} = 65.19$ GPa, and $C_{11} - C_{12} = -48.92$ GPa and $C_{44} = 26.7$ GPa. From these values, we see that both of s.c. and b.c.c. structures are unstable — even the b.c.c. structure located at the local minimum of the uniaxial loading. A shear instability always accompanies the unstressed s.c. and b.c.c. state. On the basis of present and previous discussions, we conclude that for f.c.c. Al, a stable b.c.c. structure cannot be obtained by uniaxial compression along any equivalent [001] and [111] directions. The possible Bain transformation from a stable f.c.c. to a stable b.c.c. is a branching caused by uniaxial tension.

Because of the lower symmetry under [111] loading and numerical feature of first principle

calculations, the analysis of stability under this loading mode is difficult, and is hence omitted except for the several special points, *i.e.* the initial f.c.c., unstressed s.c. and b.c.c. states. From figure 6(b), we can see that the stress and force for the uniaxial loading are always smaller than those for the uniaxial deformation. The maximum of the tensile stress is 11.05 GPa at $e_{33} = 0.295$, and the maximum magnitude of compressive stress is 15.89 GPa at $e_{33} = -0.177$. The tensile strength and critical strain are similar to those for [001] tension; however, the compressive strength and critical strain are significantly great than those for the [001] uniaxial compression. (The details are given in table 2.) This can be attributed to the symmetry of the materials. Under uniaxial compression, the stable f.c.c. crystal in the [001] case can transform to another two extreme point more easily than in the [111] case. This points is obvious from the following comparison. Under [001] loading, the stress-free b.c.c. and f.c.t. are approached at $e_{33} = -0.2$ and $e_{33} = -0.305$, where the f.c.t. structure represents the local minimum and the initial f.c.c. structure represent the overall minimum. The energy barrier from these minimums is as follows: $\Delta E_{f.c.c.\rightarrow f.c.t.} = 0.1047(\mathrm{ev/atom})$, $\Delta E_{f.c.t.\rightarrow f.c.c.} = 0.0319(\mathrm{ev/atom})$. For the [111] loading, the strain of the unstressed s.c. and b.c.c. configuration are -0.333 and -0.59, where the b.c.c. structure represents the local minimum. The corresponding energy barrier is as follows: $\Delta E_{f.c.c.\rightarrow b.c.c.} = 0.3766(\mathrm{ev/atom})$, $\Delta E_{b.c.c.\rightarrow f.c.c.} = 0.2766(\mathrm{ev/atom})$. A higher energy barrier to transition and a higher critical strain are needed for [111] compression.

VI. BIAXIAL PROPORTIONAL EXTENSION

Biaxial proportional extension is considered here. In the present paper, we deal with extension along the [010] and [001] directions; volume relaxation are not considered. The strain ratio between [010] and [001] are 0.25, 0.5 0.75 and 1. The result is given in figure 7. With increase of the ratio, the energy, stress and maximum stress increase, respectively. This is because more energy is needed with a higher transverse strain for the same longitudinal strain. However, the critical strains are similar for different proportional loading modes.

12

VII. *AB INITIO* DATABASE OF ALUMINIUM

Using total-energy calculations from first principle, Robertson *et al.* [22] and Payne *et al.* [23] constructed an *ab initio* database for aluminium, which includes 171 structures with coordination number ranging from 0 to 12 and nearest-neighbor distance ranging from 2.0 $\mathring{A}$ to 5.7 $\mathring{A}$, for fitting and testing interatomic potentials. The energies (per atom) of all structures are listed with the corresponding nearest-neighbor distances. The basic 18 structures are calculated self-consistently, and the remaining 153 structures, obtained using non-self-consistent calculations, were generated from the hydrostatic pressure. However, force, range of stability and branching points, which are important for determining the topology of energy surface, were not given in [22] and [23].

In our investigations, all of the total energy calculations are self-consistent; the basic structure is four-atoms and three-atom f.c.c. supercells; three loading modes(*i.e.* uniaxial deformation, uniaxial loading and biaxial proportional extension) and two loading directions (*i.e.* [001] and [111]) are considered. The uniaxial loading path connects structures with different coordination numbers, for example, for the [111] case, from right to left, 12 (f.c.c.)→6 (s.c.)→8 (b.c.c.), and for the [001] case, 12 (f.c.c.)→8 (b.c.c.). The complete energy and force, stress curve are plotted. In particular, the ranges of stability and branching points of [001] uniaxial loading are presented. The stabilities of three extreme points of [111] uniaxial loading are also given. These information is essential to the determination of functional form of the interatomic potential.

VIII. SUMMARY AND CONCLUSION

On the basis of DFT total-energy calculations and stability theory given by Hill and Milstein [2], [3], [7] and Wang *et al.* [13], [14], we have given a detail investigation of the mechanical response of f.c.c. aluminium for different loading modes and loading directions. We reached the following conclusions:

(1). In view of the requirement of crystal symmetry, the general form of the energy versus stretch, and stress versus stretch relations for uniaxial loading of cubic crystal can be described as follows: one local minimum, one local maximum, and one overall minimum for energy versus stretch curve, which are related with three unstressed state. The state in the middle is always unstable because of its positioning at an energy maximum.

However, when we consider the a complicated crystal, for example one with diamond structure, or alloys [38], [39], the conclusions above should be treated with caution. In such case, the symmetry is determined by both the structural parameters and the atomic ordering, and some symmetry-dictated extrema may be lost.

(2). The complete stress-strain curves for uniaxial deformation and uniaxial loading along the [001] and [111] direction, and for biaxial proportional extension are obtained. The magnitudes of the stress and force for the uniaxial deformation is always greater than those for the uniaxial loading in the [001] and [111] directions over the range of stability. The stability range for [001] uniaxial loading is given explicitly. The tensile and compressive strength along the [001] and [111] directions are presented.

(3). Along the path of [001] uniaxial loading, the local minimum, local maximum and overall minimum correspond to unstressed f.c.t., b.c.c. and f.c.c. structures; under [111] uniaxial loading, they relate to stress-free state b.c.c., s.c. and f.c.c. respectively. The intermediate b.c.c. for [001] uniaxial loading and s.c. for [111] uniaxial loading are unstable as they lie at local maximum. Although the f.c.t. state for [001] uniaxial loading and b.c.c. state for uniaxial [111] loading lie at the local minimum, they are still unstable against the shear instability. It is worthy noting that the b.c.c. configuration for the [001] and [111] loading are different configuration. Their lattice constants are $3.176\mathring{A}$ and $3.253\mathring{A}$, and the former is located at a local maximum while the later is located at a local minimum.

A stable b.c.c. state of Al metal cannot be obtained by uniaxial compression along any equivalent [001] and [111] direction. The possible Bain transformation is a branching from the prescribed path of uniaxial tension along equivalent [001] or [110] directions accompanied by branching.

(4). The tensile strength is similar along the [001] and [111] directions. For the higher energy barrier for [111] uniaxial compression, the compressive strength is greater than in the [001] case.

(5).The present results add to the existing *ab initio* database.

ACKNOWLEDGMENTS

REFERENCES

[1] M. Born, Proc. Cambridge Phil. Soc. **36**, 160(1940); M. Born and K. Huang, *Dynamical Theory of Crystal Lattices* (Clarendon, Oxford, 1956).

[2] R. Hill, Math. Proc. Cambridge Philos Soc. **77**, 225(1975).

[3] R. Hill, F. Milstein, Phys. Rev. B **15**, 3087(1977).

[4] F. Milstein and R. Hill, Phys. Rev. Lett. **43**,1411(1979).

[5] *Idem,* J. Mech. Phys. Solids **25**, 457(1977).

[6] *Idem, ibid* **26**, 213(1978).

[7] F. Milstein, in *Mechanics of Solids*, edited by H. K. Hopkins and M. J. Sewell(Pergamon, Oxford, 1982), p. 417.

[8] F. Milstein, B. Farber, Phil. Mag. A **42**, 19(1980).

[9] F. Milstein, Phys. Rev. B **3**, 1130(1971).

[10] F. Milstein, I. Appl. Phys. **44**, 3833(1973).

[11] F. Milstein, K. Huang, Phys. Rev. B, **18**, 2529(1978).

[12] F. Milstein, R. Hill, K. Huang, Phys. Rev. B **21**, 4282(1980).

[13] J. Wang, S. Yip, S. Phillpot, and D. Wolf, Phys. Rev. Lett **77**, 4182(1993).

[14] J. Wang, J. Li, S. Yip, S. Phillpot and D. Wolf, Phys. Rev. B **52** , 12627(1995).

[15] Z. Zhou, B. Joós, Phys. Rev. B **54**, 3841(1996).

[16] M. Senoo, I. Fujishiro and M. Hirano, Bull. JMSE **27**, 2680(1984).

[17] E. Espositp, A. E. Carlsson, D. D. Ling, H. Ehrenreich, C. D. Gelatt Jr., Phil. Mag. A **41**, 251(1980).

[18] A. T. Paxton, P. Gumbsch and M. Methfessel, Phil. Mag. Lett. **63** , 267(1991).

[19] M. Šob, L. G. Wang, V. Vitek, Mater. Sci. Engin. A **234 - 236** , 1078(1997); P. Šandera, J. Pokluda, L. G. Wang, M. Šob, *ibid*, A**234 - 236**, 370(1997).

[20] F. Milstein, H. Fang, anf J. Marschall, Phil. Mag. A.**70**, 621(1994).

[21] S. Fox and H. J. F. Hansen, Phys. Rev. B. **53**, 5119(1996).

[22] I. J. Robertson, D. Thomson, V. Heine and M.C. Payne, J. Phys: cond. matter. **6,** 9963 (1994).

[23] M. C. Payne, I. J. Robertson, D. Thomson and V. Heine, Phil. Mag. B, **73**,191 (1996).

[24] C. Truesdell and R. Toupin, *Handbuch der Physik*, edited by S. Flügge (Springer-Verlag, Berlin, 1960), Vol. III/1, p. 226.

[25] M. Fuchs, M. Scheffler, Comput. Phys. Commun., to be published

[26] X. Gonze, R. Stumpf, M. Scheffler, Phys. Rev. B **44**, 8503(1991).

[27] M. Bockstedte, A. Kley, J. Neugebauer and M. Scheffler, Comput. Phys. Commun. **107**, 187(1997).

[28] D. R. Hamman, Phys. Rev. B **40**, 2980(1989).

[29] N. Troullier, J. L. Martins, Phys. Rev. B **43**, 1993(1991).

[30] J. Perdew, A. Zunger, Phys. Rev. B **23**, 5048(1981).

[31] F. D. Murnaghan, Proc. Nat. Acad. Sci. U.S.A. **50**, 697(1944).

[32] G. Simmons and H. Wang, *Single Crystal Elastic Constants and Calculated Aggreated Porperties: A Handbook*, 2nd ed., MIT Press, Cambridge MA (1971).

[33] Y. Sun, E. Kaxiras, Phil. Mag. A **75**, 1117(1997).

[34] M. J. Mehl, B. M. Klein and D. A. Papaconstantopoulos, *Intermetallic Compounds: Vol. 1, Principles*, J. H. Westbrook and R. L. Fleischer, eds. (John Wiley & Sons, Ltd.,

London, 1994), Ch. 9.

[35] F. Milstein, J. Mater. Sci **15**, 1071(1980).

[36] F. Milstein, Solid. St. Commun. **34**, 653(1980).

[37] F. Milstein, B. Farber, Phys. Rev. Lett. **44**, 277(1980).

[38] P. J. Cralevich, M. Weinert, J. M. Sanchez, R. E. Watson, Phys. Rev. Lett. **72**, 3076(1994).

[39] M. Šob, L. G. Wang, V. Vitek, Comp. Materials. Sci., **8**, 100(1997).

TABLE I. Elastic moduli of Al at the equilibrium state.The length unit angstorm and T=300K with the experimental lattice constants.$C_{11} + C_{12}$, $C_{11} - C_{12}$ and C_{44} are the elastic constants of single crystal; the other moduli are for isotropic materials'.

	a_0	$C_{11}+C_{12}$	$C_{11}-C_{12}$	C_{44}	B	G	E	ν	A
Exp.(T=300K) [32]	4.05	168	46	28	76.	26.	70.	0.35	1.22
Present work(T=0K)	3.97	183	61.4	37.4					
Mehl(T=0K) [34]	3.99	184	58.	33.					
Sun(T=0K) [33]	3.95		58.8	45.5					
Present work(T=300 K)	4.05	164	44.8	28.1	74.7	25 .6	69.0	0.347	1.25
Mehl(T=300 K) [34]	4.05	150	50	31	67.	28.	75.	0.31	1.24
Sun(T=300K) [33]	4.05		45	29.7					

TABLE II. The strength of Al calculated for different loading modes; here, TS means tensile strength, and CS means compressive strength.

	Uni. Deformation	ϵ_{33} $\epsilon_{11}=\epsilon_{22}$	Uni. Loading	ϵ_{33} $\epsilon_{11}=\epsilon_{22}$
[001 TS	12.65 (GPa)	0.30, 0.	12.1 (GPa)	0.272, -0.0386
[001] CS			-5.62 (GPa)	-0.1, 0.049
[111] TS	11.52 (GPa)	0.265,0.	11.05 (GPa)	0.295, -0.0453
[111] CS			-15.89 (GPa)	-0.177, 0.110
Shear strength [18]	4.61 (GPa)			

FIGURES

FIG. 1. Two fundamental cells of the face-centred tetragonal lattice and body-centred tetragonal lattice within the same lattice

FIG. 2. The calculated strain energy (a), force and stress (b) during [001] deformation and [001] loading for the theoretical lattice constant.

FIG. 3. The calculated elastic constants (a) and stability (b) undering [001] loading for the theoretical lattice constant.
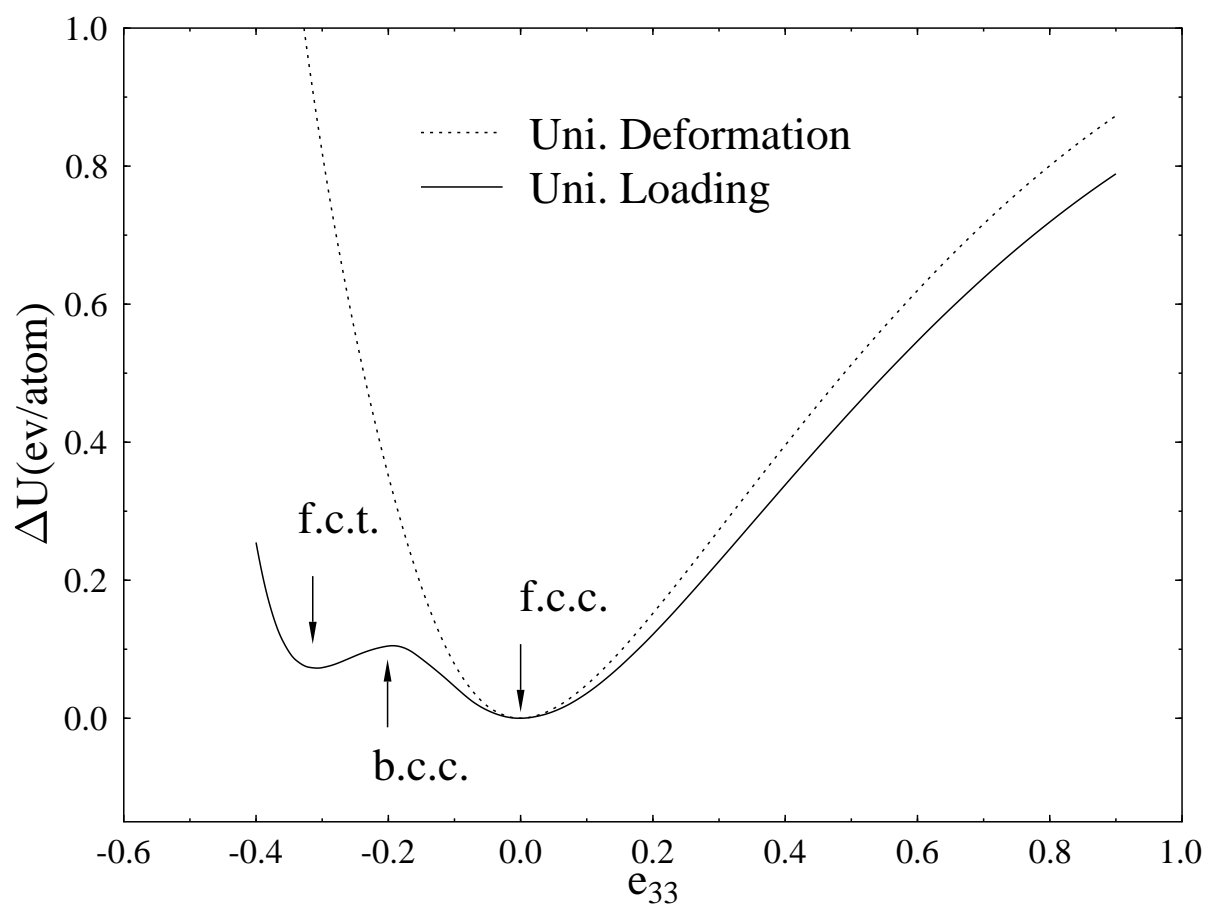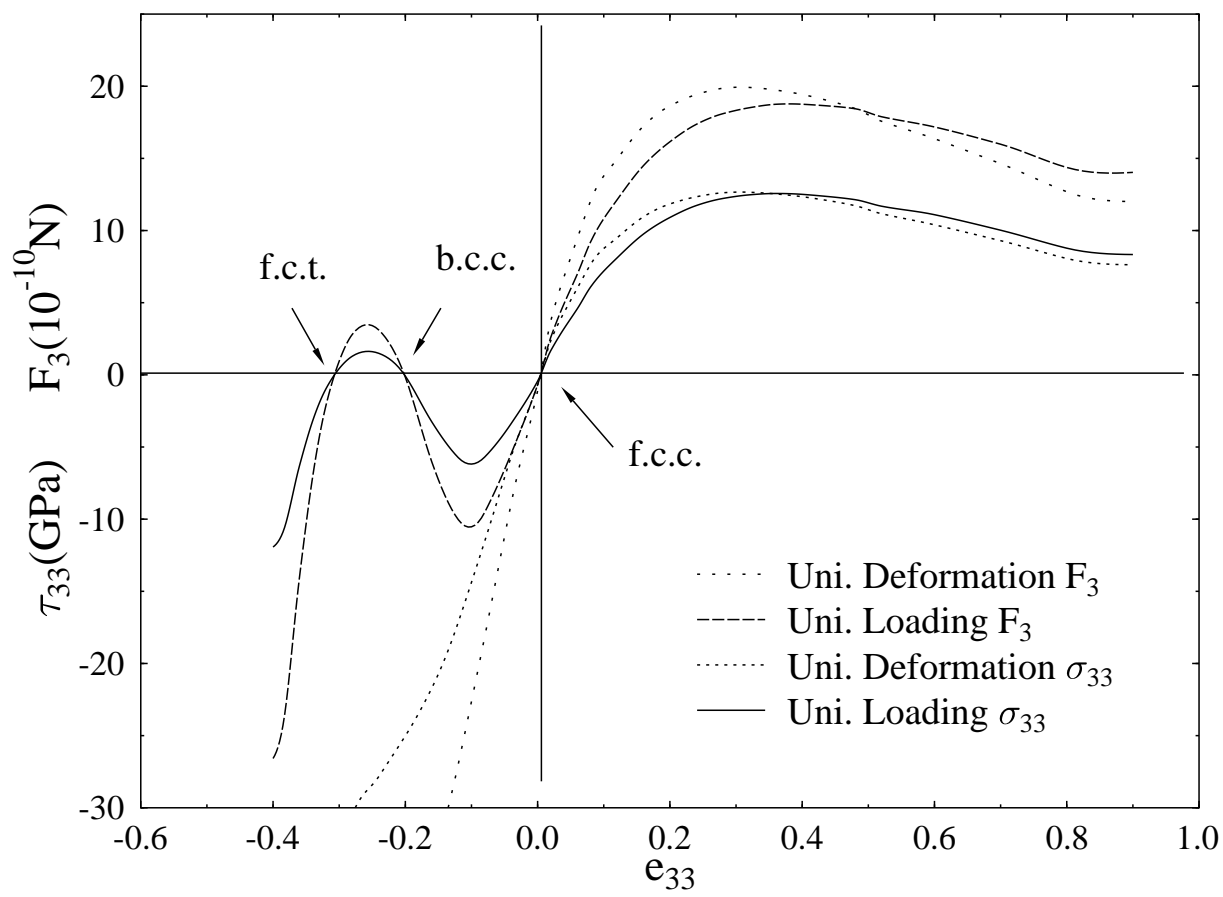
FIG. 4. The calculated transverse strain for [001] loading and [111] loading with the theoretical lattice constant.

FIG. 5. The three smallest tetrahedra cut separately from f.c.c., s.c., and b.c.c. structures. The length unit of each tetrahedron is its lattice constant of the corresponding original lattice. The bottom plane is just the {111} plane, and the triangle ABC is an equilateral triangle; the direction of OD is [111]. The ratio of OD to CB is the ratio of longitude stretch to transverse strecht.

FIG. 6. The calculated strain energy (a), force and stress (b) for [111] deformation and [111] loading with the theoretical lattice constant.

FIG. 7. The calculated strain energy(a) and stress(b) during biaxial proportional extension, with diffenerce ratio along the [010] and [001] directions, for the theoretical lattice constant.
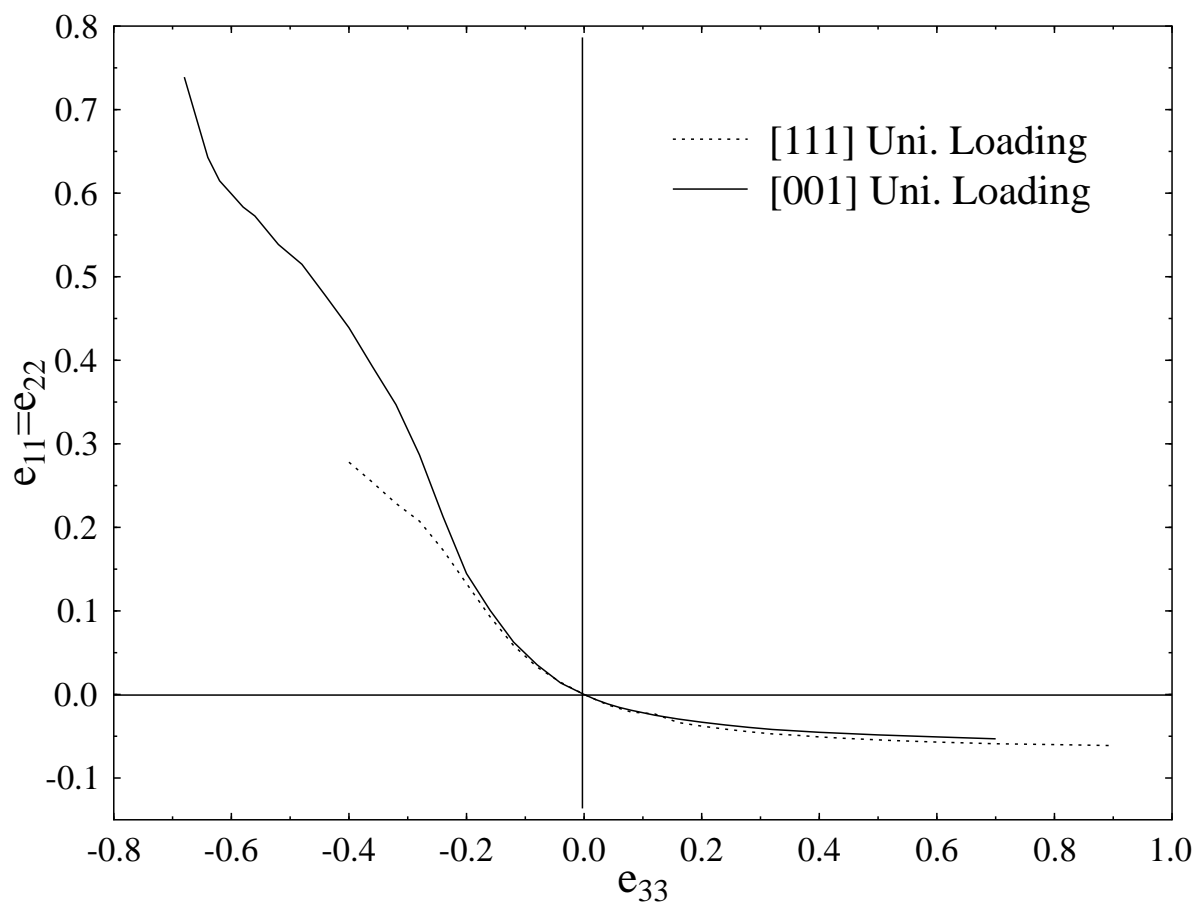
λ_3

λ_2

λ_1

(a)

(b)

(a)

Stability (GPa) vs e_{33}

Legend:
- × 10^{-2} Spindoal
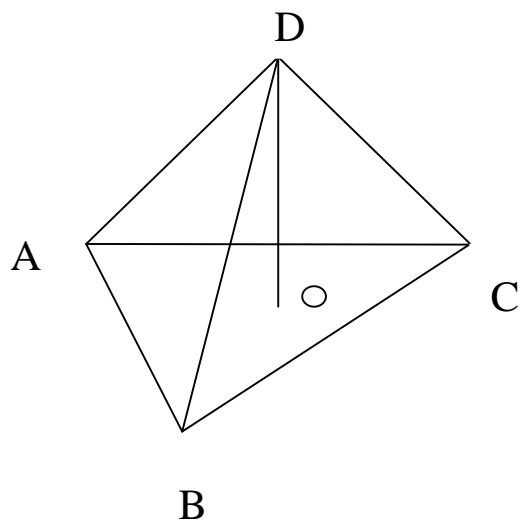- □ $C_{11}-C_{12}$
- ● $C_{44}+0.5\,\sigma$
- ♣ C_{66}
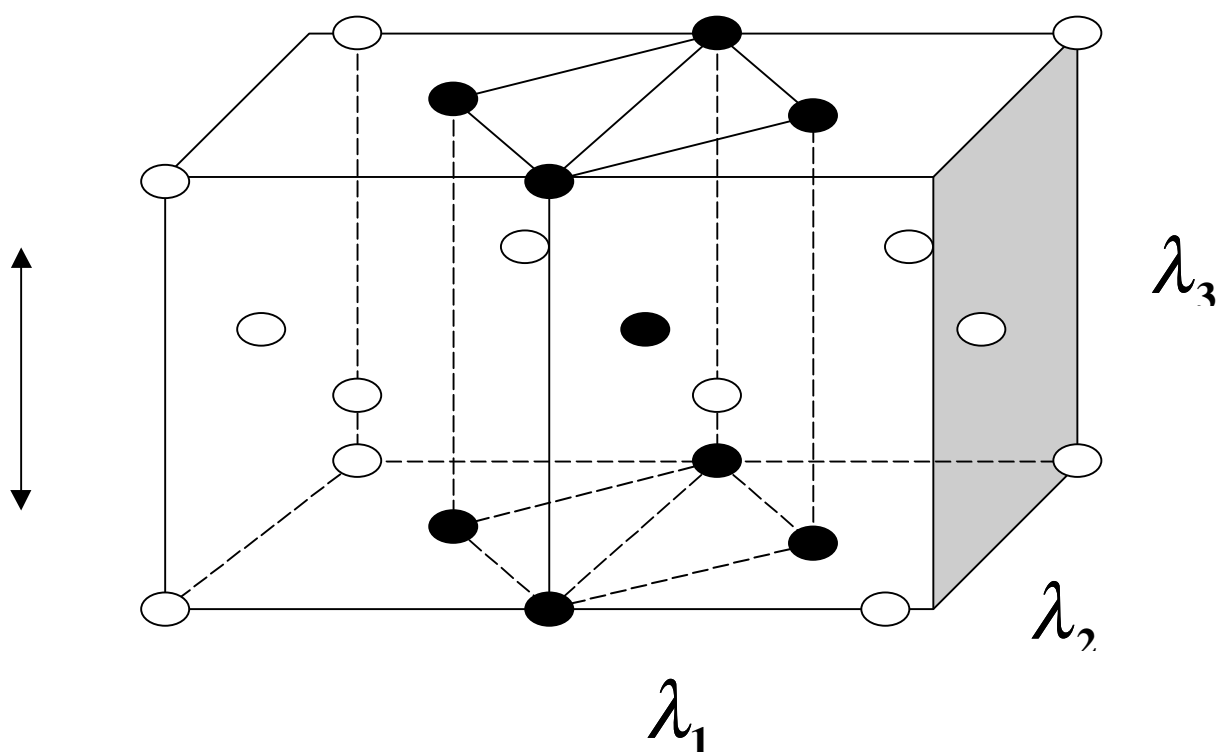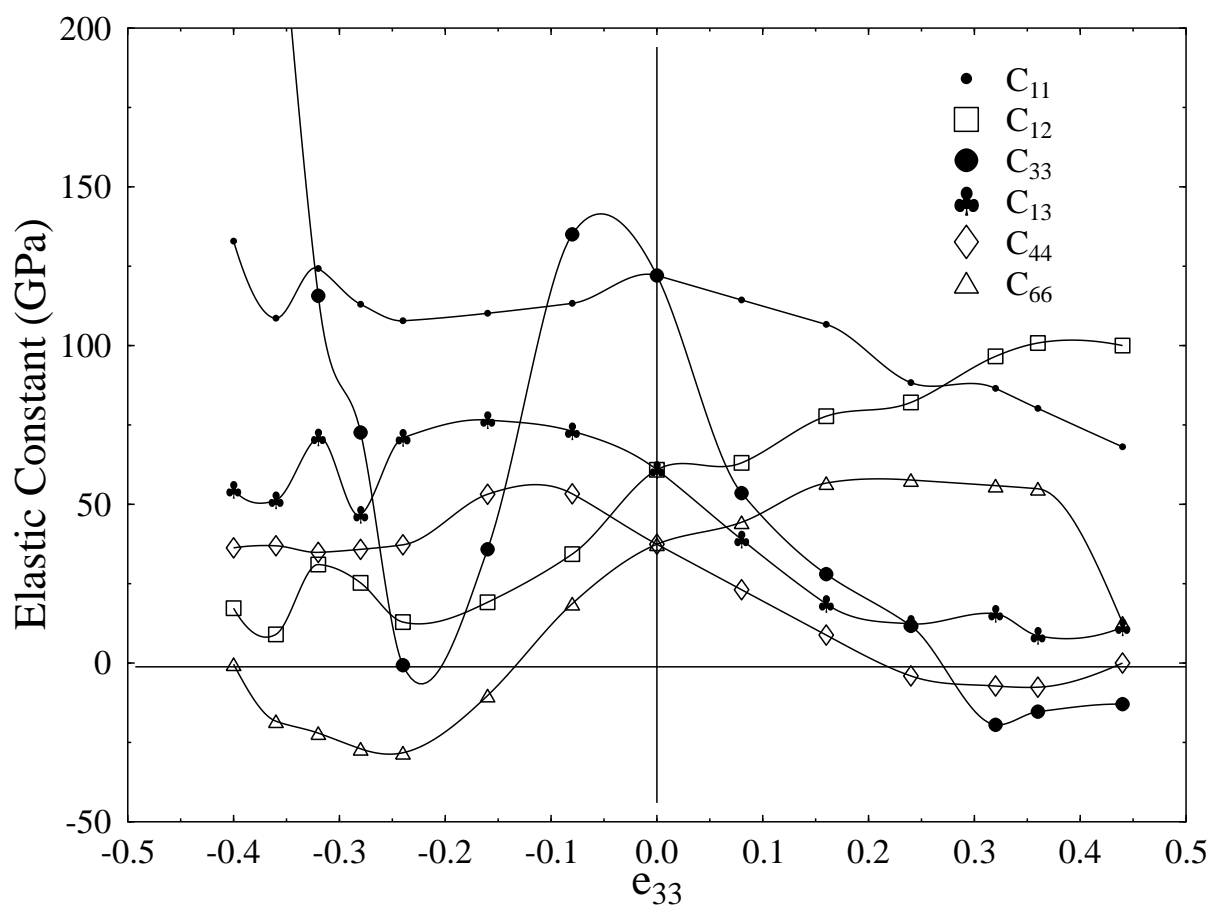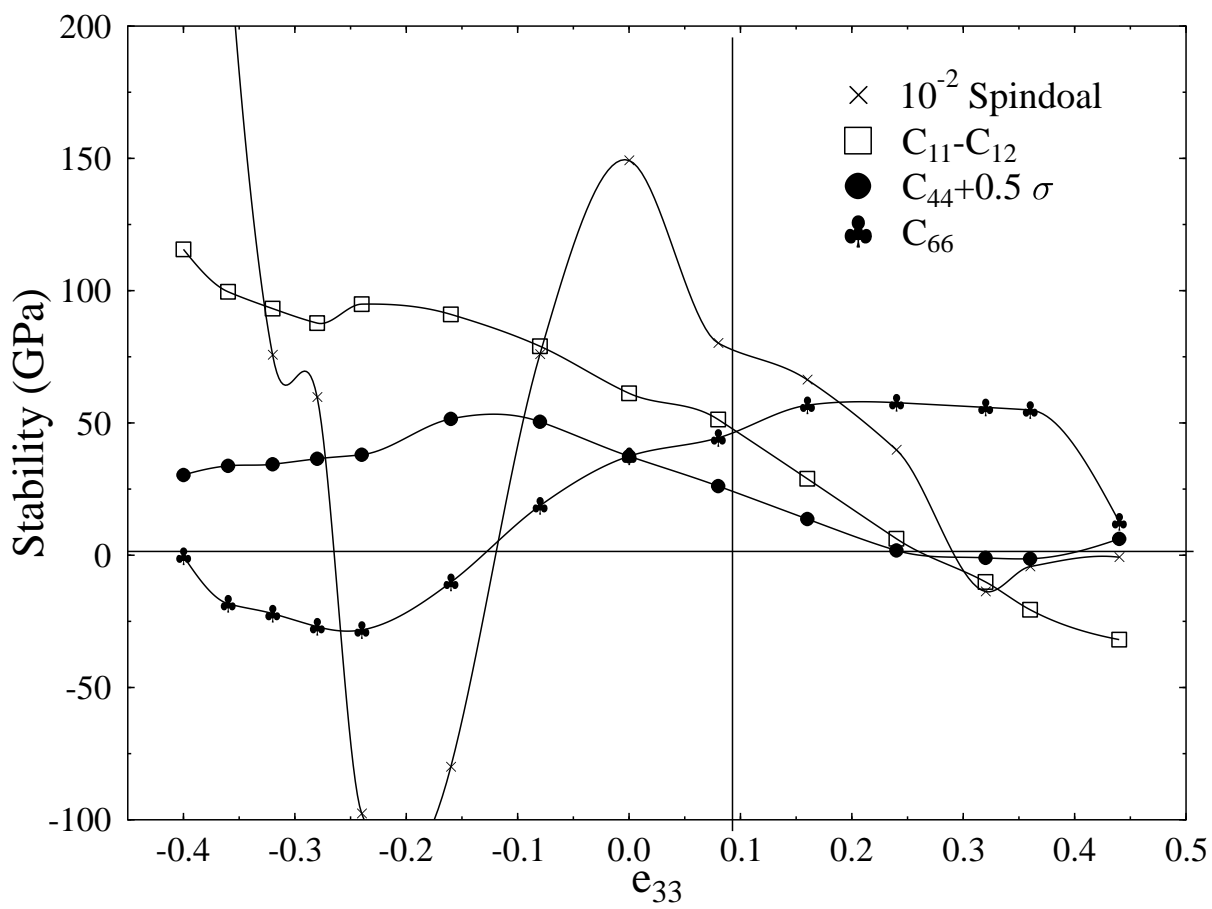
(b)
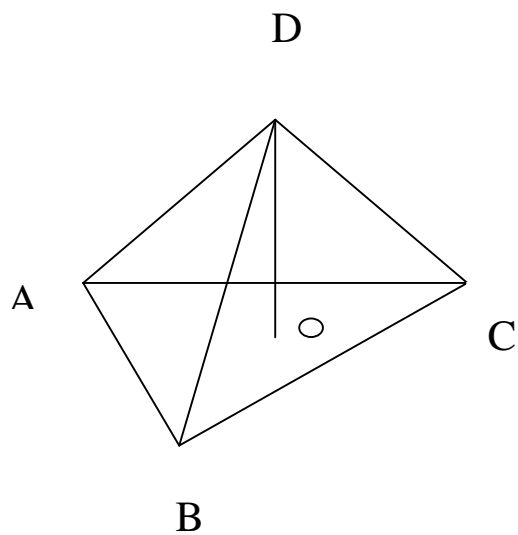
F. C. C.

$AC = BC = AB = 2^{1/2}/2$
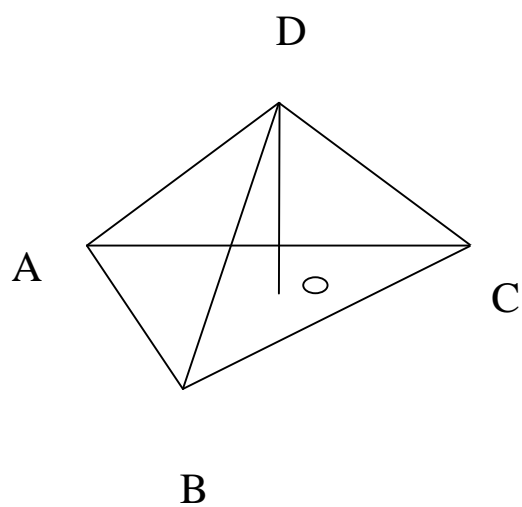
$DA = DB = DC = 2^{1/2}/2$

$DO/AB = 6^{1/2}/3$

S. C.

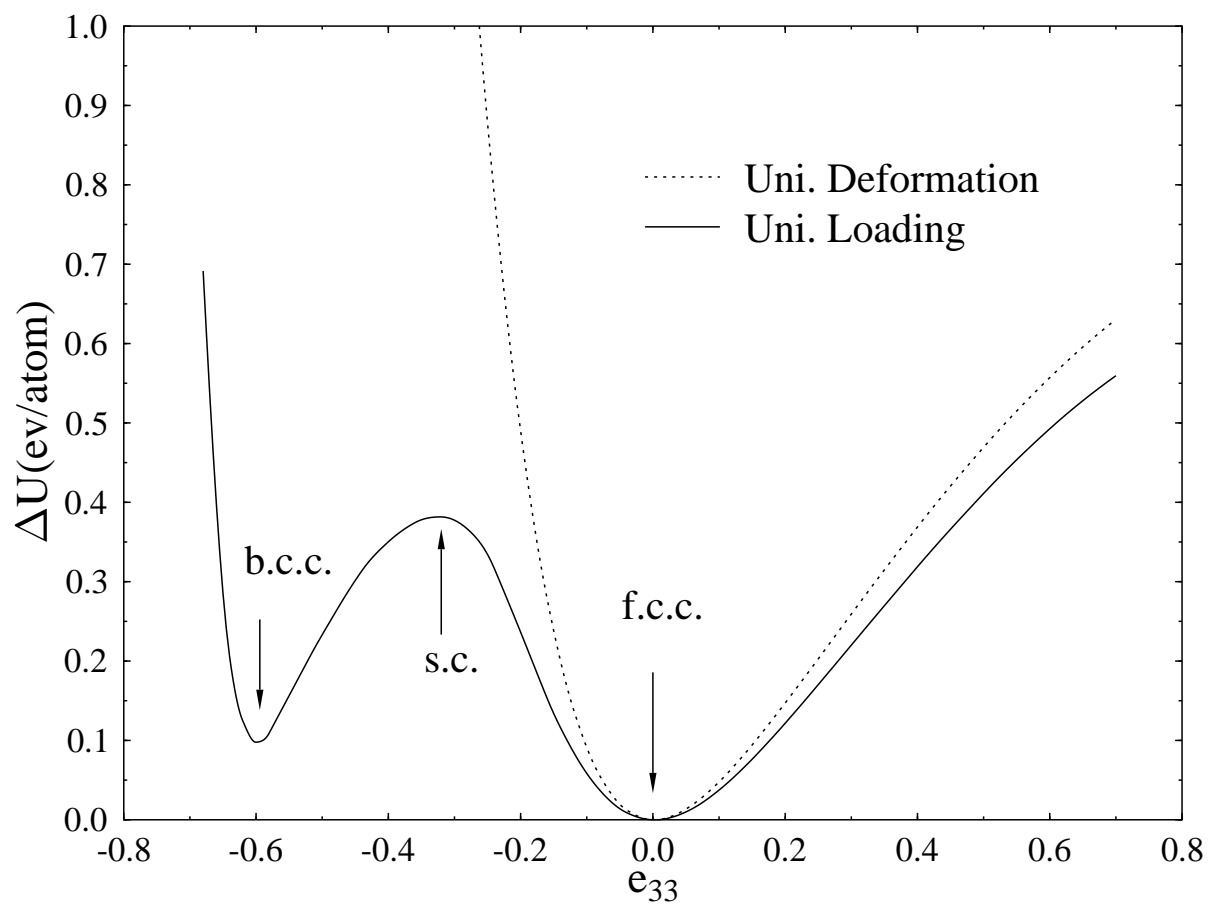$AC = BC = AB = 2^{1/2}$
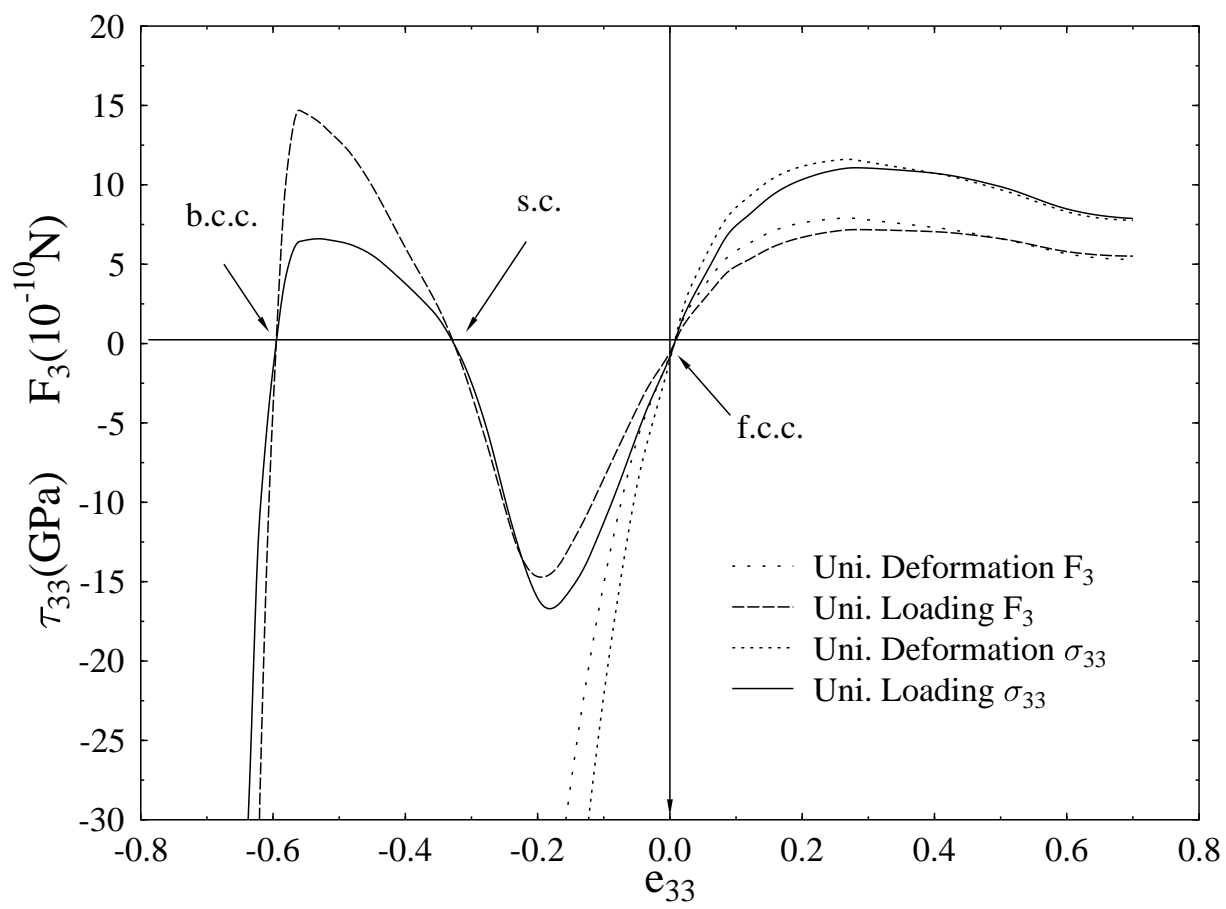
$DA = DB = DC = 1$
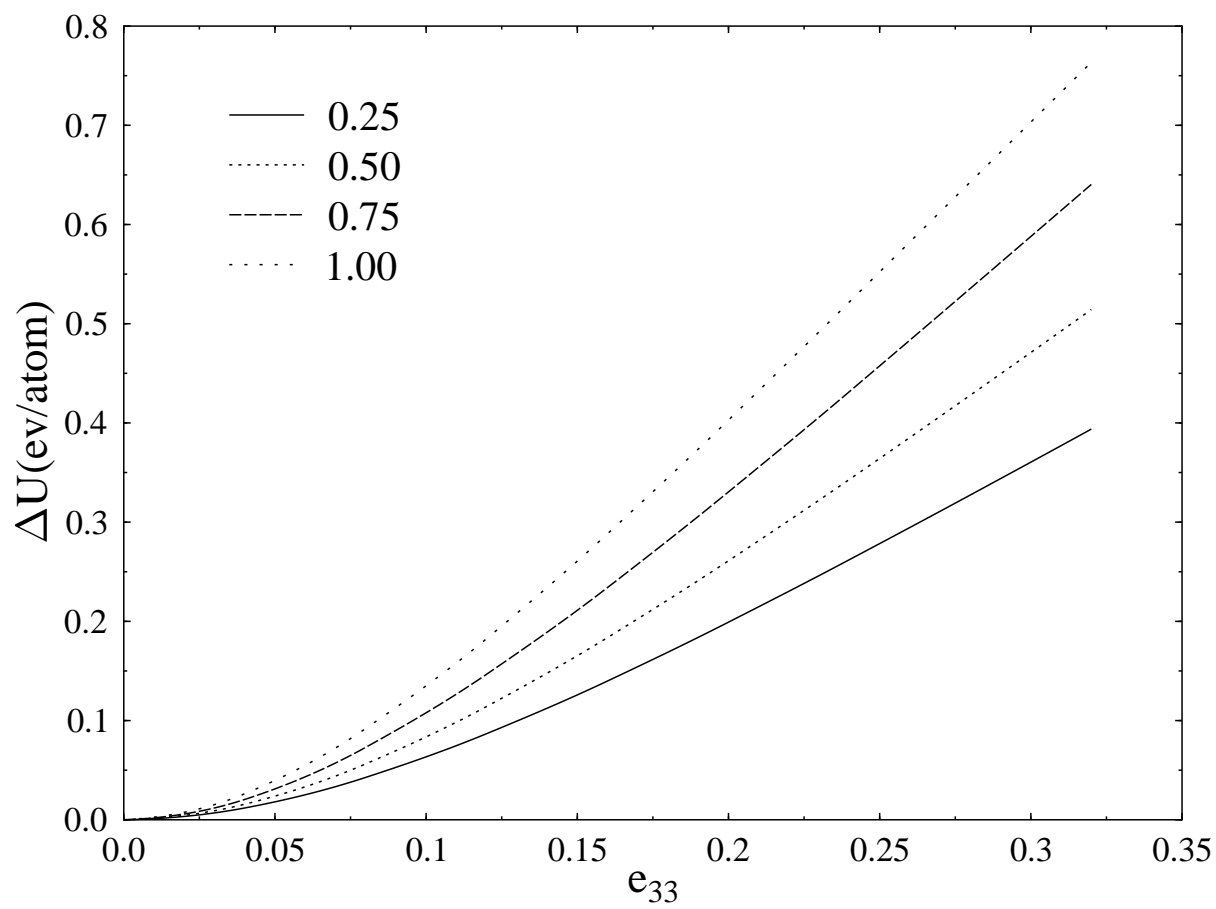
$DO/AB = 6^{1/2}/6$

B. C. C.

$AC = BC = AB = 2^{1/2}$
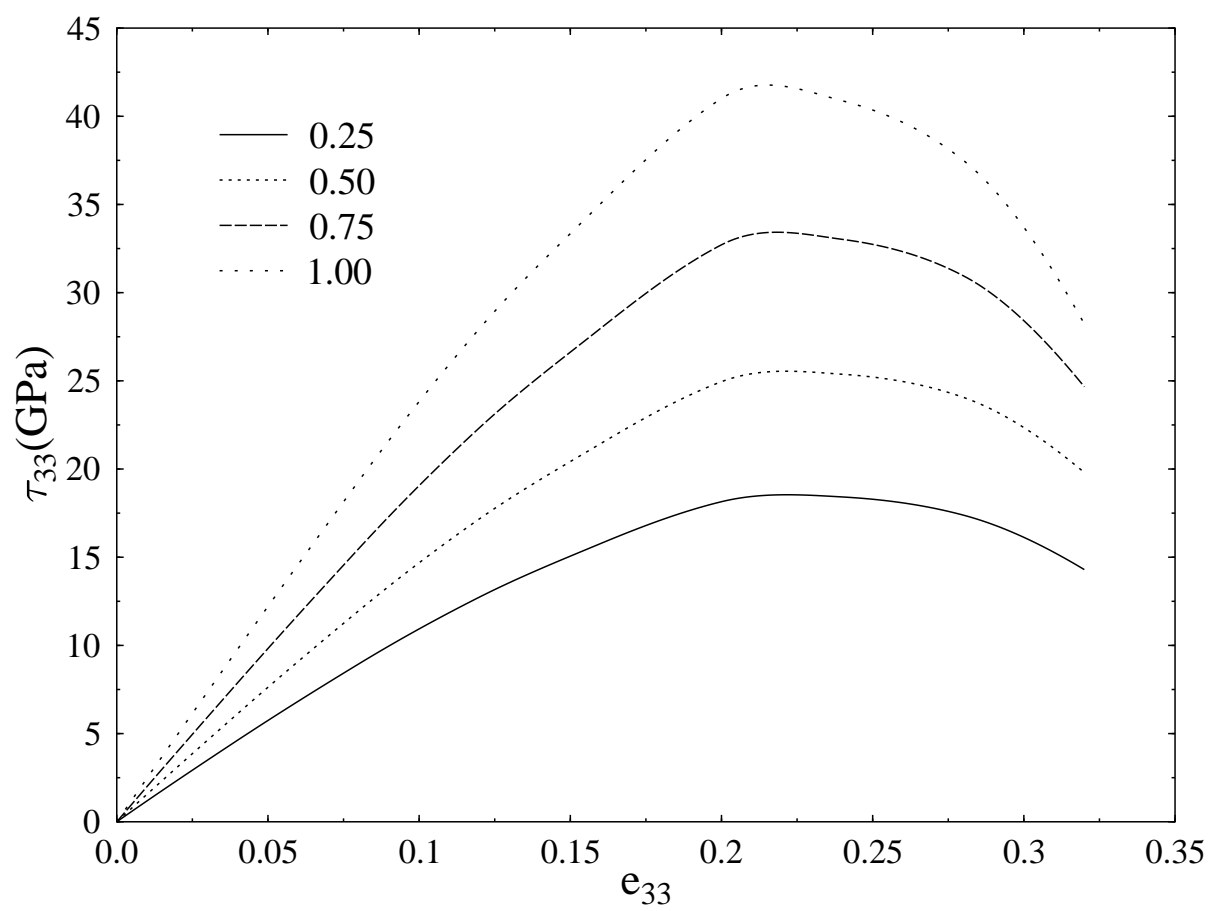
$DA = DB = DC = 3^{1/2}/2$

$DO/AB = 6^{1/2}/12$

(a)

(b)

(a)

(b)